

Design conversion, and performance estimation of BLDC motor in hybrid electric vehicle

Thenmozhi GANESAN¹ , Chandra VANARAJ² , Manoharan SUBRAMANIAN³ ,
and Radhika ALAGESAN⁴

¹ Department of Automobile Engineering, Kumaraguru College of Technology, Coimbatore, India

² Department of Electrical and Electronics Engineering, AAA College of Engineering and Technology, Sivakasi, India

³ Department of Electrical and Electronics Engineering, Thiagarajar College of Engineering, Madurai, India

⁴ Department of Electrical and Electronics Engineering, Sri Krishna College of Engineering and Technology, Coimbatore, India

Abstract. The core concept in this paper is to hybridize a conventional engine-powered two-wheeler into a hybrid electric vehicle. The shift in the consumers' mindset from conventional IC engine vehicles to electric/hybrid vehicles may be a challenge due to the high initial investment. Hence, as a preliminary work, it is proposed to convert an IC engine vehicle to a hybrid electric vehicle considering factors such as affordability, user control, and flexibility. To make the hybrid vehicle available at an affordable price, lead-acid batteries are used for the study. Also, the BLDC motor used in this vehicle was designed and developed according to the available design constraints. The moped was redesigned to operate in either engine or electric mode individually depending on the rider's desire and can switch over to any mode at any time as intended. This is achieved using a unique switching mechanism constructed using needle roller bearings. The concept of hybridization thus results in reduced emissions, especially in stop-go traffic where electric mode can be used, and the performance of hybrid electric vehicles is estimated.

Keywords: BLDC motor; hybrid moped; lead acid batteries; roller bearing switching; structural analysis.

1. INTRODUCTION

A hybrid electric vehicle (HEV) utilizes multiple power sources for propulsion. Generally, the sources are a petrol or a diesel engine and an electric motor. The primary benefits of hybrid vehicles are higher fuel economy and lesser CO₂ emission than petrol or diesel vehicles. The low popularity of hybrids, especially in India, can be attributed to the higher cost. Hybrid vehicles also have certain special features like idle start-stop system, regenerative braking, torque assist, etc. HEVs combine the power and economy of an IC engine with the higher torque and eco-friendliness of an electric power train. mopeds are always meant to be affordable and easy to maintain heavy-duty two-wheelers. Integrating a parallel or a series hybrid system into it is a daunting task. The easiest way is to leave the engine part of the vehicle untouched and to integrate an electric drive into it. The moped can be run on engine drive or electric drive individually and independently at any time but cannot be run on both at the same time. This minimizes complexity in the drive train and saves costs. A switching mechanism constructed using needle roller bearings integrated into the final drive gives the rider complete control over the selection of a power source. Such a setup ensures limited modifications to the final drive and reduces complexity and cost even further. The emissions in stop-go traffic are 25% higher compared to those at normal

riding speeds. The hybrid moped can be run in electric drive completely in these conditions which results in zero emissions, fuel savings, and higher fuel economy.

Authors [1] introduced the concept of a hybrid electric vehicle that utilizes more than two energy sources for complete vehicle propulsion. The two independent propulsion resources, the internal combustion engine (ICE) and the electrical motor, each function individually to collectively contribute to the vehicle total propulsion. The IC engine is the major source, and it is active at initial pickup and the electric motor is the supportive propulsion. The vehicle used is a Kinetic Honda Y2K Scooter. The motor used is a 48 V, 250 W, hub motor powered by five 12 V, 20 Ah lead-acid batteries through a controller. The vehicle when tested, was able to achieve an average speed of 30 km/h and a range of 55 km. The efficiency of the vehicle was boosted by a significant 25%. The suitability of such a vehicle for a country like India is being analyzed by the authors.

Harikrishna Shiyani [2] focused on fabricating a hybrid moped with an electric start and petrol run. During the "Engine Off" period the moped will run by battery power using a brushless DC (BLDC) hub motor, and by doing so it also consumes less running cost as the battery requires recharging after a long time of constant running on the motor. The system is a parallel hybrid and uses a 48 V, 250 W BLDC hub motor and four batteries of 12 V each. The combined output of the engine and BLDC motor is 2.25 kW which drives the wheels. The hub motor fixed in the front wheel can drive the vehicle to a speed of 25 km/h. The batteries have a charging time of 5–6 hours and can run for 20–25 km on a full charge. The idea

*e-mail: thenmozhi.g.auto@kct.ac.in

Manuscript submitted 2024-10-02, revised 2024-11-19, initially accepted for publication 2024-12-28, published in March 2025.

to make a bicycle that lasts longer and automatically recharges when the bicycle is not utilized by renewable solar energy has been well described by the authors [3]. A 17.6 V solar panel a 12 V controller and a 12 V battery are used. The vehicle can attain a speed of 15 km/h and a maximum range of 15 km. The hybrid bicycle is also 73% cost efficient than existing e-bikes. The cost per km is only ₹2 and the charging time takes around 4 hours through a conventional charger. The charging is possible using three sources and the system will enhance the bicycle operational efficiency. Moreover, the solar panels also have a high life span of 25 years.

Discussion on maximizing the advantages of the two power sources (petrol, electric) and minimizing the disadvantages of the same are clearly elaborated by the authors described in [4]. It also considers an attempt to make a hybrid with an electric start and petrol run. A TVS Scooty is used for this process and the front wheel hub, and the forks are altered to fix the motor. A BLDC motor of 240 W and four batteries of 48 V 20 Ah are used. The combined power output of the engine and motor propels the vehicle to a maximum speed of 22–24 km/h and a range of 34 km. The engine was found to have an efficiency of 45 km/h, and the electric mode has a range of 12 km. The cost reveals the lowest per unit distance which is found to be \$0.010. The authors focus on introducing the idea of an “eco-hybrid two-wheeler,” that integrates two systems: petrol and electric [5]. The petrol system and the electric system are designed for rear-wheel-drive and front-wheel-drive, respectively. When the vehicle is driven with petrol, the batteries get automatically charged and it uses the stored charge while running on an electric system. A 48 V, 750 W BLDC hub motor and four batteries of 12 V each are used as the main components. The overall cost of running a conventional IC engine moped and a hybrid one is found out and the cost analysis is conducted.

Authors [6] emphasized the fabrication and optimization of a two-stroke internal combustion engine automobile that operates on both the battery and gasoline. The hybrid vehicle is constructed to run using a drive powered by solar energy in addition to engine power. The solar panel attached to the scooter body is linked to the battery, which is subsequently plugged into the hub motor. A solar panel of 480 W is connected to four batteries of 12 V, 18 Ah each, and this in turn is connected to a 48 V, 350 W BLDC hub motor which propels the vehicle. The operational cost was found to be ten times less than that of a petrol-engine vehicle. The different types of hybrid vehicles were thoroughly explained by the authors Ehsani *et al.* [7] and Husain [8]. Mid-drive BLDC motors have the following advantages: high starting torque, higher efficiency, and low noise, which makes them a preferred choice for automotive applications [9]. The author [10] specified the methodology for designing a BLDC motor utilizing MagNet 7.1.1. Hence, the performance of the BLDC motor systems for EVs/HEVs is to be investigated. In this paper, modification in rotor magnet orientation, and skew angle is done, and the trapezoidal back-EMF waveform and rectangular current waveforms are analyzed. Also, the sinusoidal back-EMF waveform was studied by the authors [11, 12]. To obtain a strong mechanical structure with better performance, an interior rotor PM motor was selected [13].

Based on these reference articles, a conventional IC engine vehicle is converted into a hybrid vehicle with independent modes of operation namely IC engine mode and electrical mode. For this, a brushless DC (BLDC) motor has been designed based on the design specifications and the earlier work done by the authors Thenmozhi *et al.* [14–16]. In this paper [17], the effect of permanent magnet material selection, and its geometric properties on the cogging torque was studied by the authors using Ansys software. The flux density observed with ceramic-5 magnets was poor, but the use of Neodymium Iron Boron-35 B resulted in an increased flux density. The analysis revealed that the cogging torque diminishes as the magnet supports increase.

The authors [18] used a genetic algorithm for reducing cogging torque. Research [19] demonstrated that core materials of high grade and cost did not necessarily lead to enhanced efficiency in electric motors. This paper [20] presents an explanation of the interaction between core materials and the magnet material through the application of finite element analysis. The authors list the following challenges faced by electric scooters: efficiency, cost-effectiveness, and feature implementation, all of which are interrelated [21]. Advancements in battery technology and energy reuse will enhance the range of electric two-wheelers, while innovative designs will enable lighter, more efficient models. These cost-effective options will attract billions seeking profitable investments. The growth of the EV market in India relies on user acceptance and a shift from traditional to electric two-wheelers. The study proposed by the authors [22] analyses the factors influencing this transition using 522 samples and employs five models, including KNN, RF, ANN, and SVM, to predict user preferences for electric two-wheelers.

The Honda PCX hybrid scooter [23], a parallel system integrates an internal combustion engine and an electric motor, enhancing acceleration and fuel efficiency with reduced emissions. It allows the starter to assist the engine for about three seconds during throttle engagement, and when not in engagement, assists the starter in charging the lithium-ion battery. The Yamaha Fascino hybrid 125 [24] operates mainly on a smooth motor generator. The generator supplies electric power with smooth starting and improved acceleration. This proposed HEV article started with the introduction and the literature review of BLDC motors and hybrid electric vehicle papers. In Section 2, the design calculations of the vehicle were carried out based on which the component selection was based. Section 3 explains the electromagnetic simulation of BLDC motor based on the design constraints using MotorSolve software and the performance is studied and expressed. Section 4 includes the structural changes in the hybrid moped and its analysis. The final section elaborates on the results and discussions and finally the conclusion.

The workflow of the development of HEV is shown in Fig. 1. Based on the literature study, the power calculations are performed. The vehicle selected for conversion is a TVS XL Super moped. The moped has an engine capacity of 70 cc and its specification is shown in Table 1.

The vehicle produces a peak power of 3.5 BHP and a peak torque of 5 N-m. The vehicle has a Kerb weight of 66 kg, and it

Design conversion, and performance estimation of BLDC motor in hybrid electric vehicle

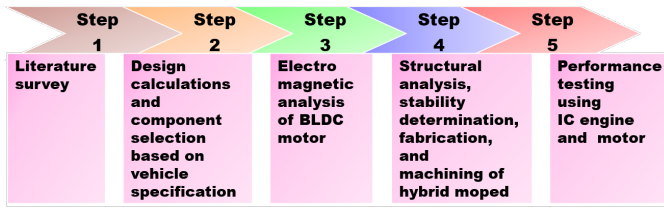


Fig. 1. Workflow

Table 1

Vehicle specifications and dimensions

Vehicle name	TVS XL Super
Engine displacement	69.9 cc
Bore × stroke	46 mm × 42 mm
Maximum power	3.5 bhp @ 5000 rpm
Maximum torque	5 N-m @ 3750 rpm
Transmission type	Automatic
Claimed fuel economy	67 km/l
Length of vehicle	2020 mm
Width of vehicle	750 mm
Height of vehicle	1110 mm
Wheelbase of the vehicle	1222 mm
Tyre size	0.4318 m
Wheel radius (r)	0.2159 m
Desired maximum speed	40 km/h

can carry a payload of 130 kg to the maximum limit. To convert into a hybrid moped, a BLDC motor with the controller, and four lead acid batteries are considered.

2. DESIGN CALCULATIONS

Kerb weight of the vehicle = 66 kg

Weight of BLDC motor = 13 kg

Weight of lead acid batteries = 80 kg

Weight of motor controller = 7 kg

Approximate weight of the rider = 90 kg

Total weight of the vehicle with rider = 256 kg

2.1. Speed and torque calculations

The design considerations assumed are (i) the road condition considered is asphalt (ii) the desired acceleration time to reach 40 km/h is 15 seconds.

$$\begin{aligned} \text{Speed } (v) \text{ in m/s} &= 40 * (1000/3600) \\ &= 11.11 \text{ m/s}, \end{aligned} \quad (1)$$

$$\begin{aligned} \text{Desired acceleration } (a) &= (v - u)/t \\ &= (11.11/15) = 0.74 \text{ m/s}^2, \end{aligned} \quad (2)$$

where u , initial velocity assumed is zero.

Let L be the linear distance travelled per rotation of the wheel

$$L = 2 * 3.14 * r = 2 * 3.14 * 0.2159 = 1.356 \text{ m}, \quad (3)$$

$$\begin{aligned} \text{Wheel RPM} &= \frac{\text{Total distance covered per hour}}{\text{Linear distance}} \\ &= \frac{(40000/60)}{(1.356)} = 492 \text{ rpm}, \end{aligned} \quad (4)$$

$$\begin{aligned} \text{Final drive ratio} &= \frac{\text{Rear wheel sprocket teeth}}{\text{Motor sprocket teeth}} \\ &= 52/13 = 4 : 1, \end{aligned} \quad (5)$$

$$\begin{aligned} \text{Rated speed} &= \text{Wheel RPM} * \text{Final drive ratio} \\ &= 492 * 4 = 1968 \text{ rpm} \\ &= 2000 \text{ rpm (approx.)}, \end{aligned} \quad (6)$$

$$\begin{aligned} \text{Force} &= \text{Mass} * \text{Acceleration} \\ &= 256 * 0.74 = 189.44 \text{ N}, \end{aligned} \quad (7)$$

$$\begin{aligned} \text{Wheel torque} &= \text{Force} * \text{Wheel radius} \\ &= 189.44 * 0.2159 = 40.9 \text{ N-m}. \end{aligned} \quad (8)$$

2.2. Force due to drag resistance (F_{dr})

The following are the assumptions and values used for calculating the drag resistance. The drag coefficient (C_d) is assumed to be 0.9, the air density (ρ) is 1.225 kg/cu.m, velocity (v) obtained is 11.1 m/s.

$$\begin{aligned} \text{Frontal area } (A) &= \text{Width} * \text{Height} \\ &= 0.75 * 1.11 = 0.83 \text{ m}^2. \end{aligned} \quad (9)$$

Rounding off to 75%,
Frontal area = 0.624 m²

$$\begin{aligned} F_{dr} &= 0.5 * \rho * C_d * A * v^2 \\ &= 0.5 * 1.225 * 0.9 * 0.624 * 11.11^2 \\ &= 42.458. \end{aligned} \quad (10)$$

Power required to overcome the drag resistance
= 42.458 * 11.11 = 470.44 Watts.

2.3. Force due to rolling resistance (F_{rr})

The coefficient of rolling resistance (C_{rr}) is 0.0127.

$$\begin{aligned} \text{Force due to rolling resistance} \\ &= m * g * C_{rr} = (256 * 9.81) * 0.0127 = 31.89, \end{aligned} \quad (11)$$

$$\begin{aligned} \text{Power required to overcome the rolling resistance} \\ &= 31.89 * 11.11 = 354.02 \text{ Watts}. \end{aligned}$$

2.4. Gradient resistance (F_{gr})

The maximum gradient assumed is 10°

$$F_{gr} = m * g * \sin \theta = 256 * 9.81 * \sin 10^\circ = 436.09, \quad (12)$$

Rated power (P) = 1261 Watts = 1.261 kW.

Rated torque

$$\begin{aligned} \text{Rated wheel torque} &= \frac{(P * 60)}{2 * \pi * N} \\ &= \frac{(1261 * 60)}{2 * 3.14 * 492} = 24.47 \text{ Nm}, \end{aligned} \quad (13)$$

$$\text{Rated torque} = \frac{\text{Rated power}}{\text{RPM}} = \frac{1261}{492} = 2.6 \text{ Nm.} \quad (14)$$

Peak power

$$\begin{aligned} \text{Peak power} &= \frac{(2 * \pi * N * T)}{60} \\ &= \frac{(2 * 3.14 * 492 * 40.9)}{60} = 2107.25 \text{ Watts} \end{aligned} \quad (15)$$

$$\text{Peak power} = 2.10 \text{ kW.}$$

Peak torque

$$\text{Peak torque} = \frac{\text{Peak power}}{\text{RPM}} = \frac{2107.25}{492} = 4.3 \text{ Nm.} \quad (16)$$

Rated current

$$\text{Rated current} = \frac{\text{Rated power}}{\text{Voltage}} = \frac{1261}{48} = 26.3 \text{ A.} \quad (17)$$

Peak current

$$\text{Peak current} = \frac{\text{Peak power}}{\text{Voltage}} = \frac{2107}{48} = 43.89 \text{ A.} \quad (18)$$

2.5. Battery calculation

Load = 1261 W

Battery specification = 48 V, 80 Ah

Battery energy = 48 * 80 = 3840 Wh

$$\begin{aligned} \text{Backup time} &= \frac{\text{Battery energy}}{\text{Load in Watts}} = \frac{3840}{1261} \\ &= 3 \text{ hours } 02 \text{ minutes} \end{aligned} \quad (19)$$

(For an 80 Ah battery, assuming the charging current to be 10% of the battery capacity).

$$\begin{aligned} \text{Battery charging time} &= \frac{\text{Battery Ah}}{\text{charging current}} \\ &= \frac{80}{8} = 10 \text{ hours.} \end{aligned} \quad (20)$$

If 20% losses are considered,

$$\text{Total charging time} = \frac{(80 + 16)}{8} = 12 \text{ hours.}$$

Note: Fast charging of the battery is also possible with the use of a 10 Amps (or) a 20 Amps fast charger.

2.6. Range calculation

Peak power output = 2107 W.

Suppose in 1 hour at 40 km/h, the power consumption is 2107 W.

$$\text{Energy consumption per km} = \frac{2107}{40} = 52.68 \text{ Wh/km.}$$

Only 80% of power can be used and 80% depth of discharge is recommended and Peukert's constant for lead acid batteries is 0.55. Peukert's constant quantifies battery capacity relative to

the discharge rate. Peukert's constant indicates the duration a battery is going to endure under a particular amount of load.

Usable energy of the battery

$$= Wh * 0.80 * \text{Peukerts constant}$$

$$= 3840 * 0.80 * 0.55 = 1690 \text{ Wh.} \quad (21)$$

Range covered with the usable energy of the battery

$$= \frac{1690}{52.68} = 32 \text{ km.}$$

The range calculated for standard environmental conditions of 1 bar pressure and 20–40°C. Optimal working temperature is 25°C for lead acid batteries. Battery life reduces by half for every 8°C rise in temperature with a corresponding decrease in range. Thus, if a 48 V 80 Ah battery and 48 V, 1500 W motor are used, it can travel at 40 km/h continuously for 32 kilometres at peak power conditions.

$$\text{Range at rated power} = \frac{1690}{31.52} = 53.6 \text{ km} = 54 \text{ km.}$$

2.7. Design-based component selection

The vehicle is capable of achieving a range of about 54 km at a constant speed at the rated power condition. It is subjected to vary depending on changes in throttle input and acceleration. From the power calculations, it was found that the maximum rated power of the motor was 1.2 kW and the maximum rated torque was 2.5 N-m. The bearing, BLDC motor, and the battery chosen for the system are given in Table 2. The battery provides a backup time of over 3 hours on rated power.

Table 2
Component specifications

Bearing specifications	
Bearing type	Needle roller bearing
Locking direction	One way
Inner diameter	12 mm
Outer diameter	16 mm
Motor specifications	
Motor type	BLDC motor
Rated power	1.5 kW
Rated torque	5 N-m
Rated current	33 A
Rated voltage	48 V
Rated speed	3000 ± 100 rpm
Battery specifications	
Battery type	Lead acid battery
No. of batteries	4
Overall voltage rating	48 V
Amp hour rating	80 Ah
Connection type	Series connection

3. ELECTROMAGNETIC ANALYSIS OF BLDC MOTOR

The motor selected for the requirement is a brushless DC motor with 48 V and a 1.5 kW power rating. Based on the previous work of Thenmozhi *et al.*, a Neodymium Iron Boron N45 grade magnet and the IPM with variable orientation [14] were chosen for the rotor design. Table 3 gives the complete details of the BLDC motor designed, simulated as in Fig. 2 and developed. To reduce the weight of the motor developed in the earlier work [8], the outer casing is redesigned and made of aluminium. The stator and rotor laminations are shown in Fig. 3. and the 3D view of the designed motor is shown in Fig. 4. Figure 5 shows the actual BLDC motor developed. Figures 6–8 represent the speed-torque characteristics, efficiency contour, and magnetic saturation, respectively.

Table 3
Motor specifications

Motor type	BLDC motor
Rated power and torque	1.5 kW, 5 N-m
Rated voltage and current	48 V, 33 A
Rated speed	3000 ± 100 rpm
Stator outer diameter	100 mm
Stator inner diameter	52.6 mm
Stator type	Square with curved tang
Stator material and thickness	35C300; 0.35 mm
No. of slots	18
No. of phases	3
Rotor type	IPM with embedded variable orientation magnets
Rotor outer diameter	51.1 mm
Rotor inner diameter	20 mm
Rotor material and thickness	35C300, 0.35 mm
No. of poles	6
Slot opening width	1 mm

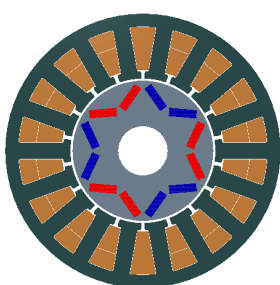


Fig. 2. Structure of 6 poles, 18 slots BLDCM with the inner rotor



Fig. 3. Laminated stator and rotor developed motor

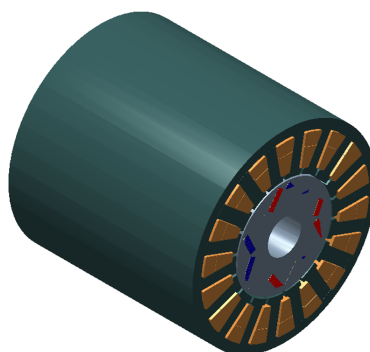


Fig. 4. 3D view of the motor using motor solve software



Fig. 5. Actual 48 V, 1.5 kW BLDC motor developed

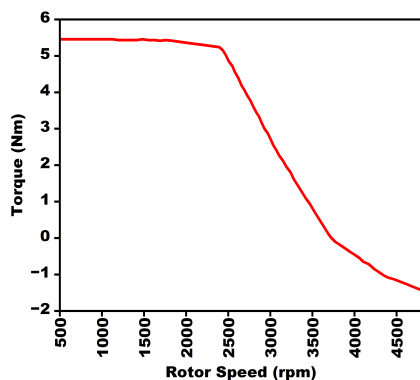


Fig. 6. Speed-torque characteristics of motor

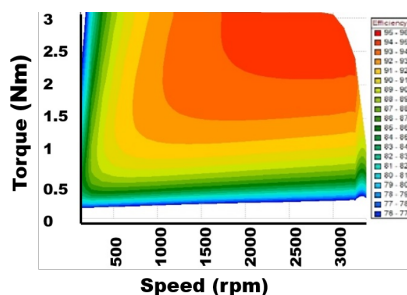


Fig. 7. Efficiency contour of the BLDC motor

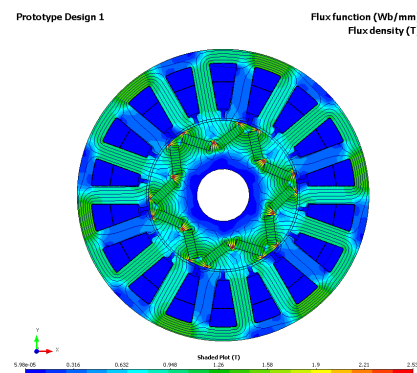


Fig. 8. Magnetic saturation of the designed motor

4. STRUCTURAL DESIGN AND ANALYSIS

The vehicle frame is modelled using CATIA V5 software. After the frame is modelled, static analysis of the frame is performed using ANSYS R22 Workbench in order to check the endurance limit of the modelled frame. The factor of safety was found to be > 1 and the stress was found to be within yield (safe) limits. The other components include a BLDC motor which has a rated power of 1500 W. The motor has a rated torque of 5 N-m. The motor has a rated voltage of 48 V and a rated current of 33 A. The motor has a peak power of 2.5 kW and a peak torque of 18 N-m. A 48 V controller is also included with the motor. Four batteries each of 12 V, 80 Ah are purchased and connected in series so that the combined voltage output of the battery system is 48 V, 80 Ah. The batteries are connected to the motor through the controller. A mechanism is provided to switch between the IC engine and pure electric mode. The pure electric mode has a range of about 32 km and a maximum operating speed of about 40 km/h. The moped has a seating capacity of one person. The components are assembled on the vehicle according to the desired configuration and fabrication of the hybrid moped is conducted.

The moped works through the use of an electric drive train and a simple cost-effective switching mechanism. The engine part of the vehicle is left untouched as no modifications are required. The electric components are fixed to the vehicle as per the location specified below. The required mounts are fabricated to hold the components in place. The chain is offset to align with the modified motor shaft. For the safety of the system and the rider, an MCB is integrated into the ignition wire of the controller. The required wiring connections are made, and the fabrication is completed. The moped is capable of running on either of the modes at a particular time depending on the convenience of the rider. The system is so designed that the moped can be run in any one of the modes at a time but cannot be run on both modes combined at the same time. This is done to reduce the complexity of the architecture. The MCB can be kept off and the vehicle can be started in engine mode and can be driven for the required distance and time. While riding in engine mode, the engine can be switched the MCB can be turned on and the vehicle can be driven in electric mode. At a time when the fuel supply is low, the vehicle can be completely driven in electric mode. The battery has to be charged separately using a fast charger.

Similarly, while the charge in the batteries is low it can be switched to engine mode. The switching mechanism ensures hassle-free engagement and disengagement within just 5 seconds. The rider thus has the flexibility to use the electric mode in the urban environments and the engine mode in the open roads thereby ensuring reduced fuel wastage and less emissions, especially in the urban environments. Also, the regenerative braking mode of operation has not been considered yet and will be implemented in future designs.

4.1. Working of a switching mechanism

The working remains the same irrespective of the mode in which the vehicle runs. Suppose if the vehicle, at the start, is turned on in engine mode, then the engine shaft rotates. As the stepped

shaft and the sprocket are coupled to the engine shaft, they also rotate. Thus, power is transmitted from the engine to the rear wheel through the sprocket and the chain as shown in Fig. 9. The power is transmitted to the sprocket as the needles in the bearing get locked together due to the rotation of the stepped shaft which is coupled to the inner diameter of the bearing. Thus, the bearing rotates, and correspondingly, the sprocket, which is coupled to its outer diameter also rotates, thus allowing power and torque transmission to the rear wheel. The sprocket which is associated with the motor drive only rotates freely on the motor shaft as the needle bearing is not locked with the stepped shaft.

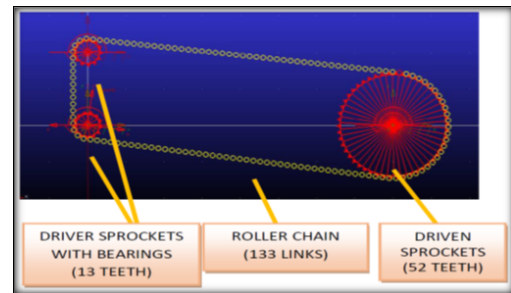


Fig. 9. Switching mechanism

The other case can also be described in the same manner where the vehicle is started in the electric mode. As the throttle is applied, the motor shaft rotates. As the stepped shaft and the sprocket are coupled to the motor shaft, they also rotate. Thus, power is transmitted from the BLDC motor to the rear wheel through the sprocket and the chain. The power is transmitted to the sprocket as the needles in the bearing get locked together due to the rotation of the stepped shaft which is coupled to the inner diameter of the bearing. Thus, the bearing rotates, and correspondingly, the sprocket, which is coupled to its outer diameter also rotates, thus allowing power and torque transmission to the rear wheel. The sprocket which is associated with the engine drive only rotates freely on the motor shaft as the needle bearing is not locked with the stepped shaft. Thus, the switching mechanism and the final drive ratio of 4:1 work together to provide a smooth and highly efficient power transmission. The construction of the mechanism eliminates unnecessary switching of the chain, thus avoiding sudden loads and ensuring a high lifetime.

4.2. Proposed structural frame design

The vehicle frame is modelled using “CATIA V5 R20” software with the dimensions measured from the vehicle. The outline of the frame sketched using the “Sketcher” module is shown in Fig. 10. and the constraints are applied to Fig. 11. Over-constraints, if any, are eliminated. The planes are offset to the required distance to sketch the mounts and the handle attachment part. A circle of diameter corresponding to the diameter of the frame is sketched at any one end of the constructed outline. The outline is then converted into 3D using the “Rib” command by selecting the profile and centre curve. The frame is then made into a hollow section using the “Shell” command. The required offset plane is selected, the outline of the handle attachment part is sketched, and the above operations are performed. The x - y

plane is offset to the required distance to construct the mount, and the outline is sketched. The mount is converted into 3D using the “Pad” command by specifying the extrusion distance. Finally, the material (Mild Steel) is applied to the completed frame model. The model is finally checked for any imperfections (or) surface overlaps (or) open profiles. The file is saved in .jigs format to import easily into the Ansys Workbench.

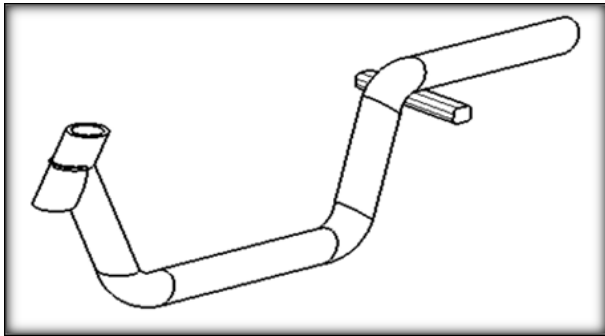


Fig. 10. Proposed frame design

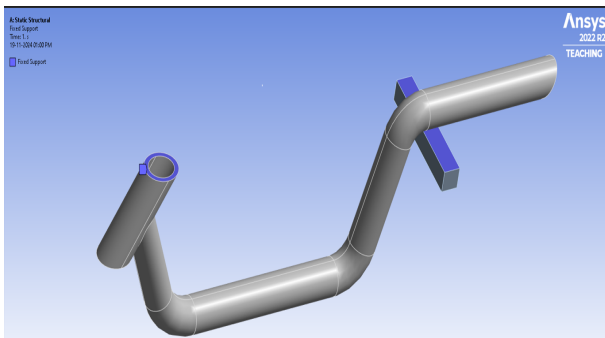


Fig. 11. Constraints – fixed supports

The material is assigned, and the meshing operation is performed on the imported geometry with the mesh size set to 5 mm. After selecting the “Generate Mesh” command, a mesh with quadrilateral elements is generated. The mesh is checked for any errors that may lead to inaccuracy in the result. If possible, the mesh is refined to the smallest element size to achieve better accuracy. The loads acting at various points of the frame are analyzed and the load value is specified in Newton. In this case, the load is given as an UDL as the load is uniformly distributed along the entire section of the frame. The frame is constrained at the mount where the suspension system is attached and at the point where the handlebar of the vehicle is attached. The constraints in the frame can be provided using a “Fixed Support.” The various forces acting at different points on the frame are to be defined next. For this definition, the “Forces” option is selected. Multiple forces can be added using the same command.

The weight of the BLDC Motor, controller, and lead acid batteries amounts to 100 kg. This weight is then converted into Newton and then applied as a uniformly distributed load on the frame as in Fig. 12. Thus, a force of 981.0 N acts in the negative z -axis direction in the part of the frame. The weight of the

rider amounts to 90 kg, 882.9 N and is applied as a uniformly distributed load on the frame. The rider’s weight is assumed to keep about a well-built person. Thus, a force of 882.9 N acts in the z -axis in the negative direction in the part of the frame shown in Fig. 13. The total weight of the internal combustion engine amounts to 30 kg. The engine weight is considered approximately as it is difficult to acquire the exact weight of the engine. This weight is then converted into Newton and then applied as a uniformly distributed load on the frame. Thus, a force of 294.3 N acts in the negative z -axis direction in the part of the frame.

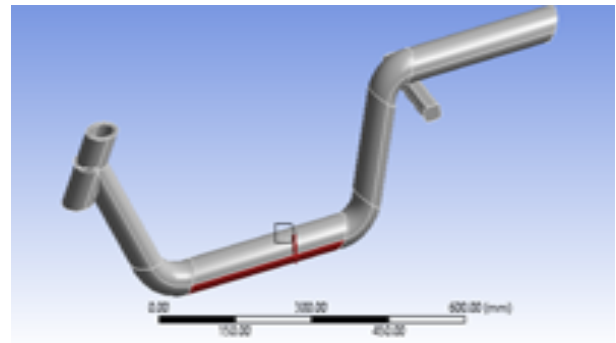


Fig. 12. Motor and batteries as a load

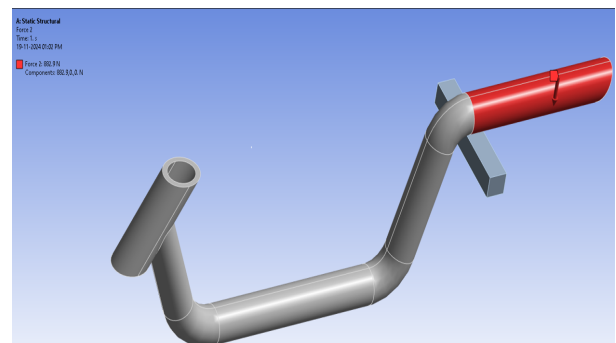


Fig. 13. Rider weight as a load

The total deformation obtained from the analysis has a maximum value of 0.1480 mm and is shown in Fig. 14. The maximum deformation was obtained at the point where the load of the rider and the batteries acts. The total deformation value obtained is very low, which indicates that the resistance of the

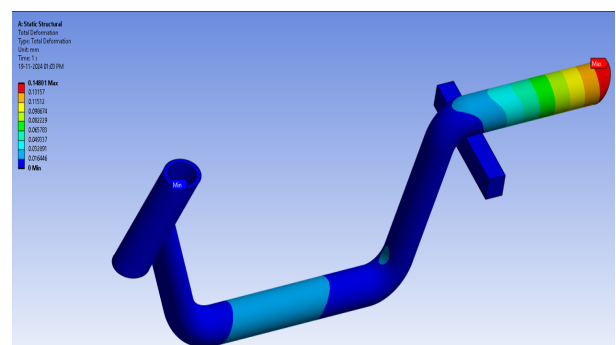


Fig. 14. Total deformation

frame to bending is greater. The minimum factor of safety (FOS) obtained from the results of the analysis was found to be 2.8386 as in Fig. 15. It is known that, for a safe design, the FOS should be > 1 . Thus, from the above analysis, it can be inferred that the frame is ultimately safe and will have a higher endurance limit. Figure 16 indicates the stress of 130.34 MPa. From the analysis, it was found that the designed frame was within the safe limits for the given loading conditions and the frame design. The frame has an exceptionally high resistance to bending as the deformation due to the added load is much lower. The frame can even withstand higher loading conditions if required. Component '1' indicates a 48 V BLDC motor, '2' indicates a 48 V motor controller, and '3' is a 48 V battery pack, which is shown in Fig. 17. The analysis of the vehicle is done using ANSYS workbench and is given in Table 4.

Table 4
 Analysis of the vehicle

Analysis type	Static structural
Software used	ANSYS workbench
Material	AISI 1018 (mild steel)
Element type	Quads
Element size	3.0 mm
Weight of motor & batteries	100 kg
Weight of rider	90 kg
Weight of engine	30 kg
Stress (Von-Mises)	130.34 MPa
Total deformation	0.1480 mm

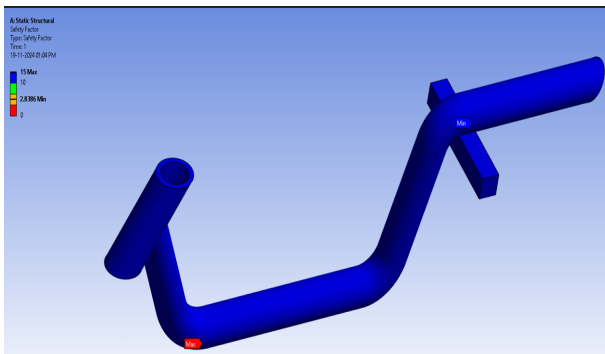


Fig. 15. Factor of safety

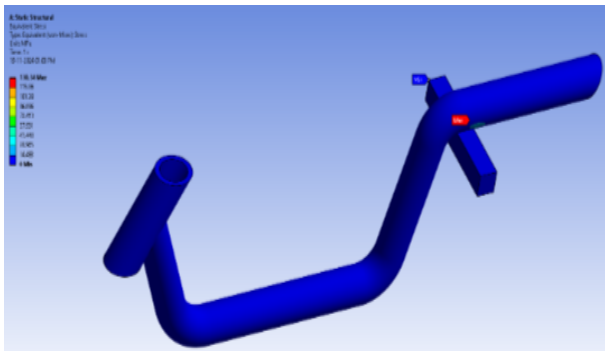


Fig. 16. Stress

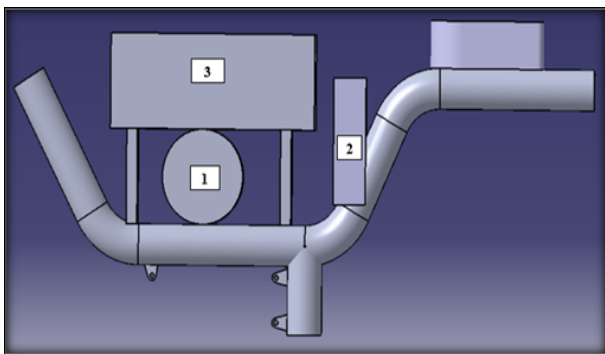


Fig. 17. Location of components

The distance of the centre of gravity from the front end of the frame in the horizontal direction (x -axis) is 434.5 mm, from the bottom end of the frame in the vertical direction (z -axis), is 303.23 mm and the condition of the vehicle-based on the position of centre of gravity is said to be stable. The location of the centre of gravity is shown in Fig. 18. Thus, the vehicle is designed, analyzed, and converted into a hybrid moped with a motor fitted as shown in Fig. 19. and the final drive in Fig. 20.

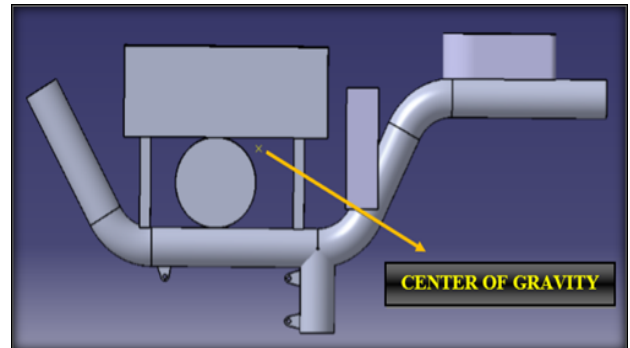


Fig. 18. Centre of gravity determination



Fig. 19. Motor fitted in the frame



Fig. 20. Final hybrid vehicle

5. RESULTS AND DISCUSSIONS

5.1. Performance test

The vehicle is tested on a two-wheeler dynamometer under laboratory conditions. Before starting the test, various factors such as tire pressures and chain tightness are checked. The vehicle is mounted on the dynamometer and the front wheel of the vehicle is locked. The rear wheel of the vehicle should be such that it must be placed on the roller. The vehicle details are entered into the dynamometer and the fuel supply line from the tank is turned off and fuel is fed to the carburetor from the small tank in the dynamometer. The vehicle is initially started in the IC engine mode and the various steps are followed as specified in the dynamometer. From the various tests, the top speed of the vehicle, acceleration, braking distance, and efficiency are found. The readings are tabulated in Table 5. The vehicle is then turned off and the fuel line from the tank is connected to the carburetor.

Table 5
Performance test results

Name of test	Engine mode	Electric mode
Top speed	65 km/h	54 km/h
Acceleration (0–40 km/h)	7 seconds	4.67 seconds
Range/fuel economy	64.5 km/l	29.8 km/full charge
Braking (from top speed)	49.40 meters	44.14 meters

The vehicle is then started in the electric mode and the testing procedure in the two-wheeler chassis dynamometer is repeated. The top speed, acceleration, braking distance, and efficiency in the electric mode are obtained. The readings are tabulated and compared to the readings obtained in the IC engine mode. This gives the difference between theoretical and experimental values in both modes. The efficiency and acceleration figures are higher in electric mode compared to the conventional IC engine mode. This is because the electric motor has a high amount of starting torque which helps in better acceleration compared to an IC engine which has to be spun to a particular rpm to access the available peak torque. The results obtained from the

performance test are tabulated below. The test is performed at standard lab conditions using a two-wheeler chassis dynamometer of double-roller type.

5.2. Cost estimation

The cost estimation of the vehicle in both modes is given below. The estimation is done on a daily travelling basis with a distance of 80 km and 24 working days a month.

Petrol mode

$$\text{Approximate cost of petrol} = \text{Rs. } 100 = \$1.19,$$

$$\text{Real-time mileage} = 50 \text{ km},$$

$$\text{Distance to be travelled daily} = 80 \text{ km (assumed)},$$

$$\begin{aligned} \text{Average consumption} &= \frac{\text{Distance travelled}}{\text{Mileage}}, \\ &= \frac{80 \text{ km}}{50 \text{ km/l}} = 1.6 \text{ litres}, \end{aligned} \quad (22)$$

$$\text{Cost of running 80 km daily} = 1.6 \text{ liters} * \text{Rs. } 100$$

$$= \text{Rs. } 160 = \$1.90,$$

$$\text{Total monthly expenditure} = 24 * 160 = \text{Rs. } 3840$$

$$= \$1.90 * 24 = \$45.6.$$

Electric mode

$$\text{Battery pack capacity} = 48 \text{ V} * 80 \text{ Ah} = 3.84 \text{ kWh.}$$

$$\text{Real-time electric mode range} = 29 \text{ km.}$$

$$1 \text{ kilowatt-hour} = 1 \text{ unit of electric energy.}$$

$$\text{Energy consumption on a full charge} = 3.84 \text{ units.}$$

Considering charger efficiency and other losses, four units are needed.

$$\begin{aligned} \text{Electricity usage per km} &= \frac{\text{Energy consumption}}{\text{range}} \\ &= 4 \text{ units}/29 \text{ km} \\ &= 0.138 \text{ unit/km.} \end{aligned} \quad (23)$$

$$\text{Maximum cost of domestic electricity} = \text{Rs. } 4.7 \text{ per unit}$$

$$= \$0.056 \text{ per unit,}$$

$$\begin{aligned} \text{Total cost of running 1 km} &= 4.7 \text{ Rs./unit} * 0.138 \text{ unit/km} \\ &= 0.648 \text{ Rs./km} = 0.0077 \text{ \$/km,} \end{aligned}$$

$$\text{Cost of travelling 80 km daily} = 0.648 \text{ Rs./km} * 80$$

$$= \text{Rs. } 51.88 = \$0.618,$$

$$\text{Total monthly expenditure} = \text{Rs. } 51.88 * 24$$

$$= \text{Rs. } 1245.3 = \$14.84,$$

$$\text{Total cost in petrol mode to travel 1920 km} = \text{Rs. } 3840$$

$$= \$45.6,$$

$$\text{Total cost in electric mode to travel 1920 km} = \text{Rs. } 1245$$

$$= \$14.84,$$

$$\text{Difference in costs between two modes} = \text{Rs. } 3840 - \text{Rs. } 1245$$

$$= \text{Rs. } 2595 = \$30.76.$$

6. CONCLUSION

The vehicle fabricated here is a prototype and can further be refined both aesthetically and mechanically. BLDC Motor simulations are done with Motorsolve software, and the vehicle analysis is done with Ansys based on which the vehicle has been converted into a hybrid vehicle. The performance test results obtained using a two-wheeler chassis dynamometer imply that the hybrid moped has a range of 30 km in the electric mode for a full charge. The acceleration time required for the vehicle in electric mode is less when compared to engine mode. Further, flexibility in usage is also available due to the independent working of the two modes. The moped is easy to maintain and use. Further, with the upcoming emission norms, the vehicle can be used completely in electric mode, and during charge depletion, an IC engine can be used. The existing IC engine two-wheelers can also be converted into a hybrid with the implementation of such systems with more concentration on regenerative braking. The concept can further be made into a product through localization and putting it into mass production if there is a surge in demand. This work mainly attempts to convert the available IC engine into a hybrid vehicle with certain constraints not considered like the increased lead acid battery weight and this could be sorted out by replacing it with lithium batteries and all the state of charge and state of health estimation studies could be made in near future.

ACKNOWLEDGEMENTS

The authors thank the Kumaraguru College of Technology India, for granting permission to use Motorsolve Software. Also, special thanks and acknowledgements to G. Hariharan, S. Sreeram, T. Vinothkumar, K. Rajkumar, and V. Nikil.

FUNDING

The authors did not receive any funds for this work.

FUTURE WORK

The authors would like to extend and modify the work to size and weight reduction of the BLDC motor with the same design requirements. Further, they would like to build a vehicle with a switched reluctance motor and compare the performance of the two motors in all aspects.

REFERENCES

- [1] N. Sharada Prasad, and R. Nataraj, "Design and Development of hybrid electric two-wheeler suitable for Indian road conditions," *Int. J. Electr. Electron. Data Commun.*, vol. 2, no. 9, pp. 60–62, 2014. [Online]. Available: https://iraj.in/journal/journal_file/journal_pdf/1-80-140965836659-62.pdf
- [2] H. Shiyani, "Efficient Hybrid Moped," *Int. J. Sci. Res.*, vol. 4, no. 11, pp. 178–180, 2015, doi: [10.36106/IJSR](https://doi.org/10.36106/IJSR).
- [3] P. Kadi and S. Kulkarni, "Hybrid Powered Electric Bicycle," *Int. J. Sci. Res. Develop.*, vol. 4, no. 5, pp. 1017–1020, 2016.
- [4] G. Adinarayana, Ch. Ashok Kumar, and M. Ramakrishna, "Fabrication of Hybrid Petro electric Vehicle," *Int. J. Eng. Res. Appl.*, vol. 4, no. 10, pp. 142–144, 2014.
- [5] G. Bansal, S. Chadha, S. Gupta, and R. Gupta, "Eco Hybrid Scooter," *Adv. Mater. Res.*, vol. 1077 pp. 185–190, 2014, doi: [10.4028/www.scientific.net/AMR.1077.185](https://doi.org/10.4028/www.scientific.net/AMR.1077.185).
- [6] S. Nataraju Prem Singh and C. Raghavendra Prasad, "Fabrication and Development of Hybrid Vehicle (scooter)," in *Proc. National Conference on Advances in Mechanical Engineering Science*, May 2016, pp. 219–222.
- [7] M. Ehsani, Y. Gao, and A. Emadi, *Modern electric, hybrid electric, and fuel cell vehicles*, 2nd Edition, CRC Press, 2010, pp. 19–65, doi: [10.1201/9780429504884](https://doi.org/10.1201/9780429504884).
- [8] I. Husain, *Electric, and hybrid vehicles: design fundamentals*, 1st Edition, CRC Press, 2003, pp. 17–39, doi: [10.1201/9780429490927](https://doi.org/10.1201/9780429490927).
- [9] V. Kamaraj, J. Ravishankar, and S. Jeevananthan, *Emerging solutions for e-Mobility and Smart Grids. 2020*, Singapore: Springer, 2021, doi: [10.1007/978-981-16-0719-6](https://doi.org/10.1007/978-981-16-0719-6).
- [10] C. Carunaiselvane and S. Jeevananthan, "Generalized procedure for BLDC motor design and substantiation in MagNet 7.1.1 software," in *Int. Conf. on Computing, Electronics and Electrical Technologies (ICCEET)*, India, 2012, pp. 18–25, doi: [10.1109/ICCEET.2012.6203783](https://doi.org/10.1109/ICCEET.2012.6203783).
- [11] K.U. Devi and M.Y. Sanavullah, "Performance analysis of exterior(outer) rotor permanent magnet brushless DC (ERPMBLDC) motor by finite element method," in *3rd International Conference on Electronics Computer Technology*, India, 2011, pp. 426–430, doi: [10.1109/ICECTECH.2011.5941785](https://doi.org/10.1109/ICECTECH.2011.5941785).
- [12] Y.C. Wu and B.W. Lin, "Computer-aided design of a brushless DC motor with exterior-rotor configuration," *Comput. Aided. Des.*, vol. 9, no. 4, pp. 457–469, 2012, doi: [10.3722/cadaps.2012.457-469](https://doi.org/10.3722/cadaps.2012.457-469).
- [13] R. Krishnan, *DC Motor Drives Permanent Magnet Synchronous and Brushless DC Motor Drives*. Taylor & Francis Group Thames, UK, 2010.
- [14] G. Thenmozhi *et al.* "Design, fabrication and performance estimation of BLDC motor for electric vehicles," in *AIP Conf. Proc.*, vol. 2869, no. 1, p. 030030, 2023, doi: [10.1063/5.0168256](https://doi.org/10.1063/5.0168256).
- [15] G. Thenmozhi, A. Radhika, and B. Mithun, "A simulation-based investigation on the Performance of BLDC motor used in Electric Vehicles for varied magnetic materials," in *8th International Conference on Advanced Computing and Communication Systems (ICACCS)*, India, 2022, pp. 875–879, doi: [10.1109/ICACCS54159.2022.9785117](https://doi.org/10.1109/ICACCS54159.2022.9785117).
- [16] G. Thenmozhi, S. Sivakumar, B. Arun, M. Nirmala, and A. Radhika, "An investigation on the performance of permanent magnet brushless DC motor based on different materials," in *AIP Conf. Proc.*, vol. 2446, no. 1, p. 100004, 2022, doi: [10.1063/5.0108137](https://doi.org/10.1063/5.0108137).
- [17] M. Yildirim, H. Kurum, D. Miljavec, and S. Corovic, "Influence of Material and Geometrical Properties of Permanent Magnets on Cogging Torque of BLDC," *Eng. Technol. Appl. Sci. Res.*, vol. 8, no. 2, pp. 2656–2662, April 2018, doi: [10.48084/etasr.1725](https://doi.org/10.48084/etasr.1725).
- [18] V. Sarac, "Performance optimization of permanent magnet synchronous motor by cogging torque reduction," *J. Electr. Eng.*, vol. 70, no. 3, pp. 218–226, 2019, doi: [10.2478/jee-2019-0030](https://doi.org/10.2478/jee-2019-0030).

Design conversion, and performance estimation of BLDC motor in hybrid electric vehicle

- [19] S.O. Kwon, J.J. Lee, B.H. Lee, J.H. Kim, K.H. Ha, and J.P. Hong, "Loss distribution of three-phase induction motor and BLDC motor according to core materials and operating," *IEEE Trans. Magnet.*, vol. 45, no. 10, pp. 4740–4743, 2009, doi: [10.1109/TMAG.2009.2022749](https://doi.org/10.1109/TMAG.2009.2022749).
- [20] M. Przybylski, B. Ślusarek, and J. Gromek, "Brushless DC motor with a bonded permanent magnet and powder magnetic core," in *Proc. XIX International Conference on Electrical Machines – ICEM 2010*, pp. 1–4, doi: [10.1109/ICELMACH.2010.5608078](https://doi.org/10.1109/ICELMACH.2010.5608078).
- [21] A.K. Nayak, B. Ganguli, and P.M. Ajayan. "Advances in electric two-wheeler technologies," *Energy Rep.*, vol. 9, pp. 3508–3530, 2023, doi: [10.1016/j.egy.2023.02.008](https://doi.org/10.1016/j.egy.2023.02.008).
- [22] M. Murugan, and S. Marisamynathan, "Mode shift behaviour and user willingness to adopt the electric two-wheeler: A study based on Indian road user preferences," *Int. J. Transport. Sci. Technol.*, vol.12, no. 2, pp. 428–446, 2023, doi: [10.1016/j.ijst.2022.03.008](https://doi.org/10.1016/j.ijst.2022.03.008).
- [23] Overview of PCX HYBRID's Hybrid System, Honda. [Online]. Available: https://global.honda/en/tech/Hybrid_System_PCX_HYBRID/ (Accessed: 12. Nov. 2024).
- [24] S. Susvirkar, "Yamaha Fascino 125 Hybrid: Road Test Review," Bikewale. [Online]. Available: <https://www.bikewale.com/expert-reviews/yamaha-fascino-125-hybrid-road-test-review/> (Accessed: 12. Nov. 2024).